



Inverted Pendulum Control using Adaptive Manifold Immersion (Part-II: Digital Implementation)

Ahmed Riaz, Muhammad B. Riaz, Abdullah, Syed S. Sajjid

Department of Electrical Engineering, COMSATS Institute of Information Technology, Wah-47040, Pakistan

Abstract This article describes a novel digital controller design for the inverted pendulum system using nonlinear adaptive immersion method. The full order system is compensated by a controller designed for a reduced order exosystem, which has a robust stabilizing performance against the given full order system. The controller design relies upon the immersion to attractive submanifold. The system dynamics are reviewed. The experimental validation of theoretically proposed continuous time controller is presented by implementing discrete time realization of control algorithm using digital controller, interfaced in the real time with MATLAB/Simulink. The actual hardware results, obtained using rapid control prototype operation of the system, are elucidated and compared with the simulated results. The viability of the proposed controller is theoretically and experimentally demonstrated by the promising behavior of the system, starting from any initial condition and hence, guaranteeing the wider operating region of the system.

Keywords Inverted Pendulum, Immersion, Invariance, Robust Adaptive Control, Rapid Control Prototyping, Digital Control

Introduction

The inverted pendulum platform is among challenging control systems. This platform has been a benchmark to practice various control techniques. A lot of research work has been dedicated to this system owing to highly nonlinear and complex dynamic structure of this system. The literature addresses techniques such as standard linearization approaches, decoupled neural network reference compensation techniques, Lyapunov function methods, computer vision-based control, adaptive fuzzy controls, H^∞ based controls etc. [1, 2]. Since most of the real-world systems are non-linear with parameter uncertainties, so most of the aforementioned techniques result in performance degradation with the parameter uncertainties and also impose the narrow operating range constraints [3, 4]. One solution to this problem is sliding mode control [5]. Sliding mode control involves the development of discontinuous control laws that make the dynamics of a system evolve on an attractive sliding manifold [6]. Moreover, sliding mode algorithm requires sliding surface to be reached [4]. We have modified and extended the continuous control algorithm, which does not necessarily require target submanifold to be reached and it is robust against parameter uncertainties as compared to optimal control approach [7] that intrinsically suffers the drawback of deterioration in system performance with plant parameter uncertainties.

We have adopted this approach to define an exosystem evolving on a submanifold in the state space of the plant. This subspace contains the zero equilibrium of the plant. A control algorithm has been presented that makes the this submanifold attractive for the full order system. The continuous time control algorithm along with the simulation results have been presented in part I of this work. However, the availability of cheap microprocessors with the immense digital processing capabilities shifts the trends towards the digital implementation of the developed control algorithm [8, 9]. On these grounds, the control of inverted pendulum using DSP and FPGA has also been considered [10]. The performance enhancement also requires to evaluate the effects of the change



of the system parameters in the real-time, in order to select the most suited system performance [11]. Hence, we also have presented a digital rapid control prototyping (RCP) mode of operation of our system that enables us to tune the controller parameters in the real-time. The closed loop responses of the digital implementation of system using ARM cortex processor, interfaced in the real time with Simulink, are presented and elucidated.

Review of the System Dynamics

The plant consists of an inverted pendulum in the form of a rod. A cylindrical mass is attached to one end of this rod and the other end is hinged to a cart capable of moving back and forth on a railing by means of a pulley-belt mechanism. The pulley is rotated by a PMDC motor. The experimental setup is shown in Figure 1.

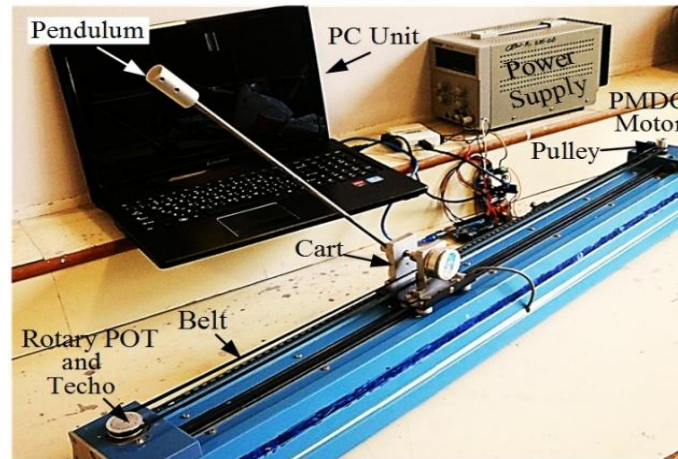


Figure 1: The experimental setup

The position and velocity of the cart are measured by rotary potentiometer and tachometer respectively, coupled to the belt as shown in Figure 1. The acceleration \ddot{x} of the cart is measured by an accelerometer on an inertial measurement unit (IMU) board attached to the cart. The pendulum angle θ and the angular velocity $d\theta/dt$ are measured by a rotary potentiometer and a MEMS rate gyro respectively, attached to the axle at the hinge of the pendulum base as shown in Figure 2.

As explained in part I of this work, let's define state vector for system as:

$$\underline{p} = [p_1 \quad p_2 \quad p_3]^T = [\dot{x} \quad \theta \quad \dot{\theta}]^T \quad (1)$$

We can describe our system in the form of Equation 2 that is suitable for geometric nonlinear control approach.

$$\dot{\underline{p}} = \underline{f}(\underline{p}) + \underline{g}(\underline{p})u = \underline{s}(\underline{p}, u) \quad (2)$$



Figure 2: The sensing mechanism



Using Equation 1 and Equation 3, the dynamics of our systems are restated in Equation 3 using work in part I of this article.

$$\begin{aligned}\underline{f}(\underline{p}) &= [0 \quad p_3 \quad k_1 \sin p_2]^T \\ \underline{g}(\underline{p}) &= [1 \quad 0 \quad -k_2 \cos p_2]^T \\ \underline{s}(\underline{p}, u) &= [u \quad p_3 \quad k_1 \sin \theta - k_2 u \cos \theta]^T\end{aligned}\quad (3)$$

Here, $u \in U(\underline{p})$ is the system forcing function, U is a state dependent input set which belongs to the control bundle $u \in \bigcup_{p \in P} U(\underline{p})$.

Adaptive Manifold Immersion

Continuous Time Controller Design

The continuous time controller designed using adaptive manifold immersion is restated in Equation 4 using work in part I of this article.

$$\begin{aligned}\mathcal{G} &= \mathcal{G}_n / \mathcal{G}_d \\ \mathcal{G}_n &= -\alpha (p_1 - \gamma_1 p_2 - \gamma_2 p_3 - 2\gamma_3 p_2 p_3) + (\gamma_1 + 2\gamma_3 p_3) p_3 + (\gamma_2 + 2\gamma_3 p_2) k_1 \sin p_2 \\ \mathcal{G}_d &= 1 + (\gamma_2 + 2\gamma_3 p_2) k_2 \cos p_2\end{aligned}\quad (4)$$

The partial state feedback law is restated in Equation 5.

$$e_a = \frac{1}{a_6} [(a_1 + a_2 \sin^2 p_2) u - a_3 p_3^2 \sin p_2 + a_4 \sin(2p_2) + a_5 p_1] \quad (5)$$

3.2 Digital Controller Design

The control algorithm in Equation 4 and the partial state feedback law in Equation 5 are discretized with the sampling time $T = 0.1$ sec and $k = nT$ resulting in Equation 6 and Equation 7 respectively. The issues related to discretization e.g. mathematical elaboration of effects of sampling time are a part of the future work.

$$\begin{aligned}e_a[k] &= \frac{1}{a_6} [(a_1 + a_2 \sin^2(p_2[k])) u[k] - a_3 (p_3[k])^2 \sin p_2[k] \\ &\quad + a_4 \sin(2p_2[k]) + a_5 p_1[k]]\end{aligned}\quad (6)$$

$$\begin{aligned}\mathcal{G}[k] &= \mathcal{G}_n[k] / \mathcal{G}_d[k] \\ \mathcal{G}_n[k] &= -\alpha (p_1[k] - \gamma_1 p_2[k] - \gamma_2 p_3[k] - 2\gamma_3 (p_2[k])(p_3[k])) \\ &\quad + (\gamma_1 + 2\gamma_3 p_3[k])(p_3[k]) + (\gamma_2 + 2\gamma_3 (p_2[k])) k_1 \sin(p_2[k]) \\ \mathcal{G}_d[k] &= 1 + (\gamma_2 + 2\gamma_3 (p_2[k])) k_2 \cos(p_2[k])\end{aligned}\quad (7)$$

Simulation of Digital Controller

The digital control algorithm in Equation 6 and Equation 7 is simulated in the Matlab/Simulink as shown in Figure 3.

The state space trajectories of system are presented in Figure 4. It is clear that off the manifold dynamics decay out with time and system converges to the invariant submanifold shown in this figure, however, the submanifold is not invariant, which is the case for continuous time counterpart. The trajectories pass through the manifold but ultimately converge to it, owing to the attractivity of the submanifold. The pendulum angle and velocity are plotted in the Figure 5 and Figure 6 respectively, and both converge to zero. The cart position and velocity are plotted in Figure 7 and Figure 8 respectively. It is evident that these dynamics are stable. The off-the-manifold dynamics are plotted in Figure 9. These dynamics decay with time towards zero, hence proving that this submanifold is attractive. The feedback linearized input and PMDC motor input voltages are plotted in Figure 10 and Figure 11 respectively. These values are realizable and within the practical limits.



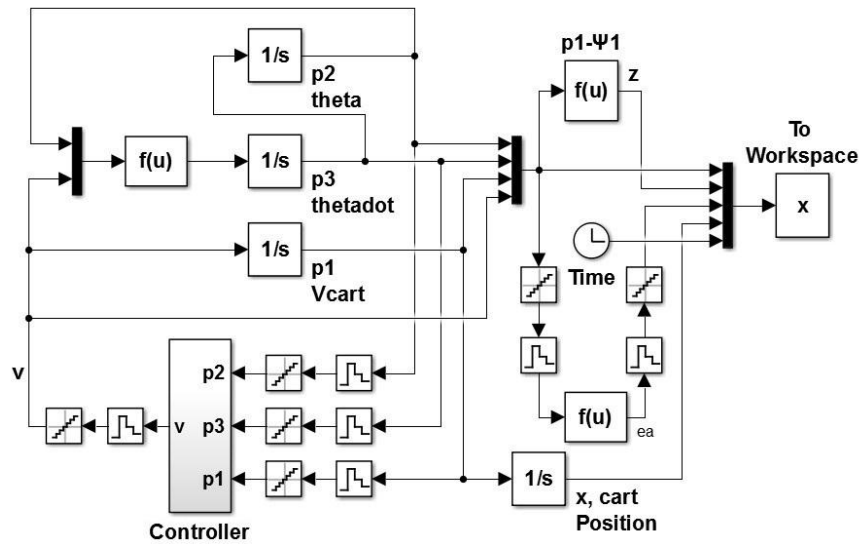


Figure 3: Digital Control algorithm simulation

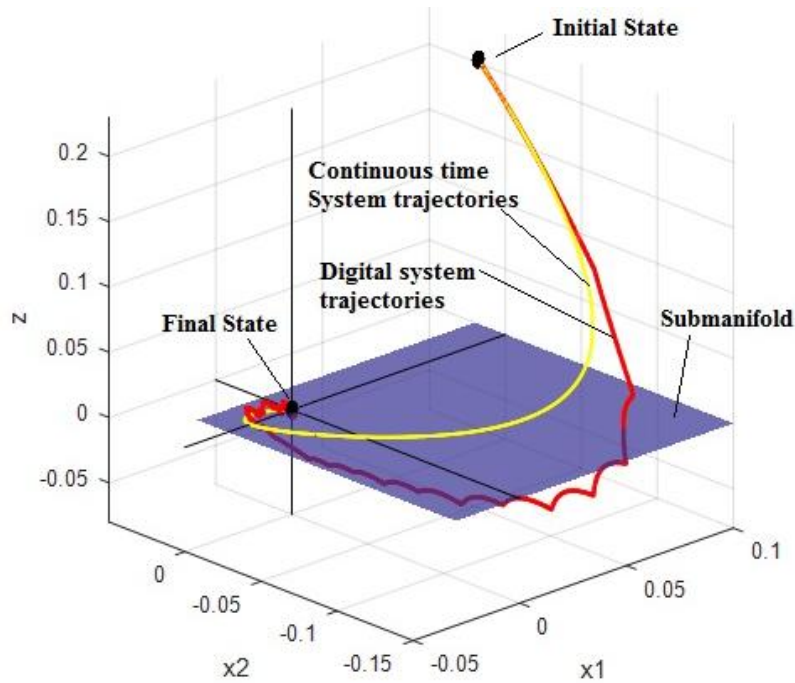


Figure 4: System trajectories and immersion submanifold

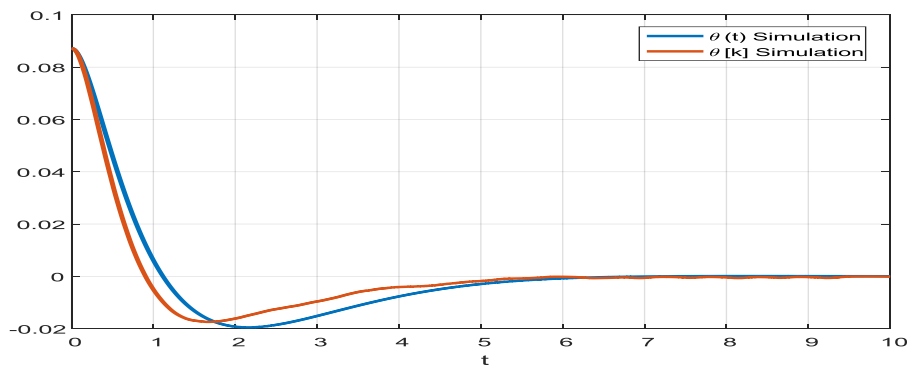


Figure 5: Responses for pendulum angle θ .

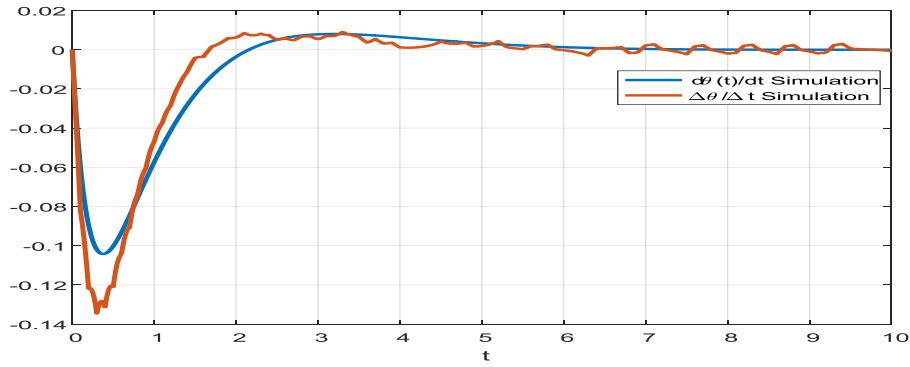


Figure 6: Responses for pendulum angular rates.

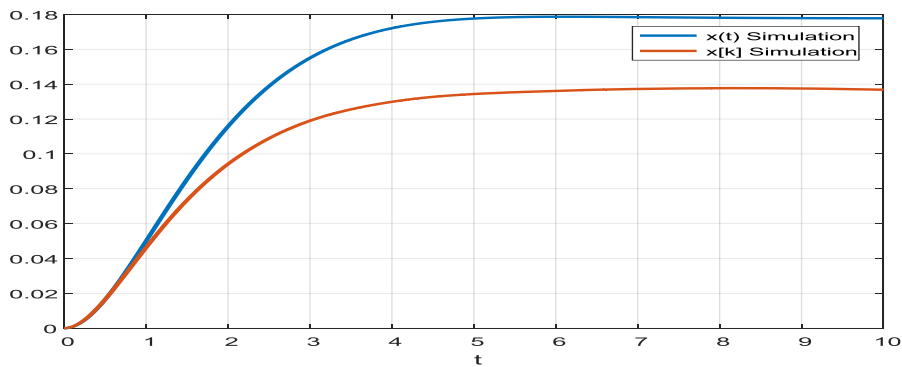


Figure 7: Responses for cart position x .

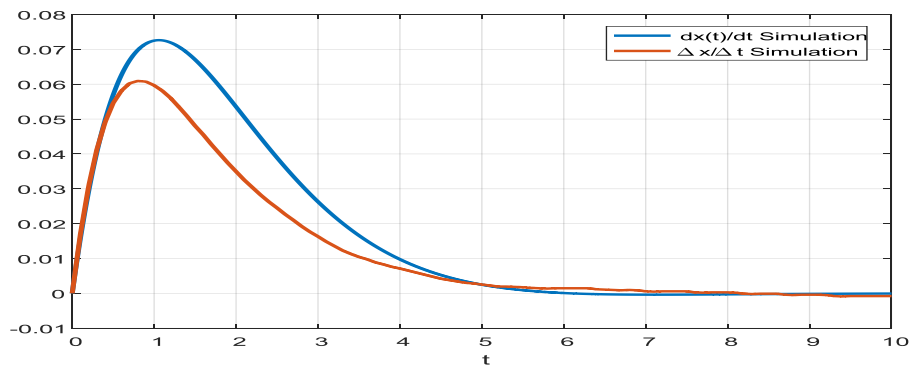


Figure 8: Responses for the cart velocity

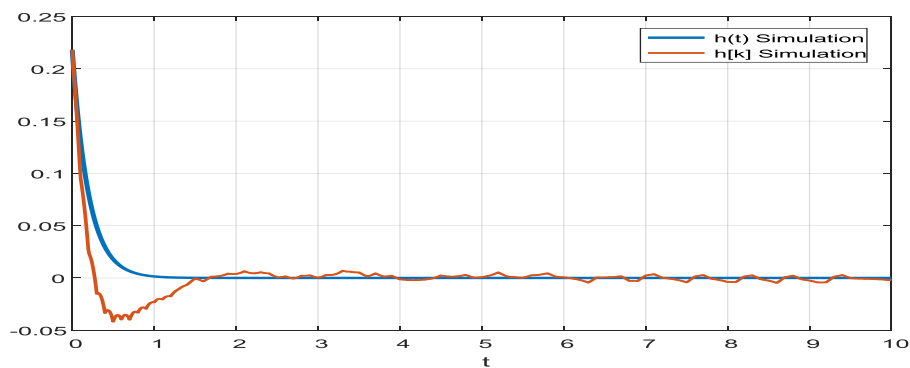
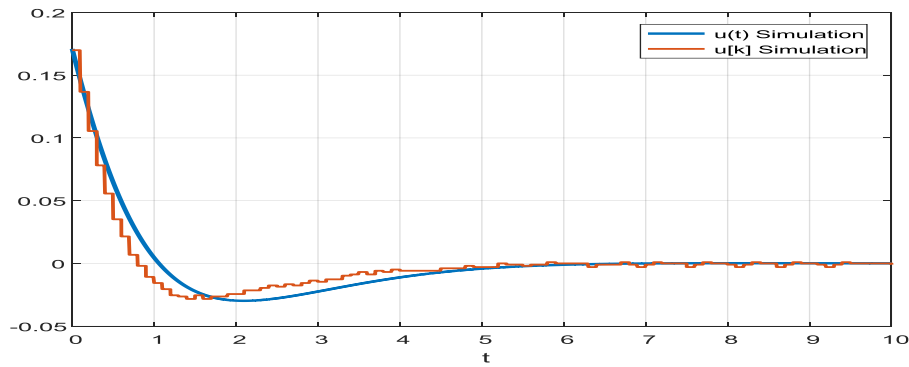
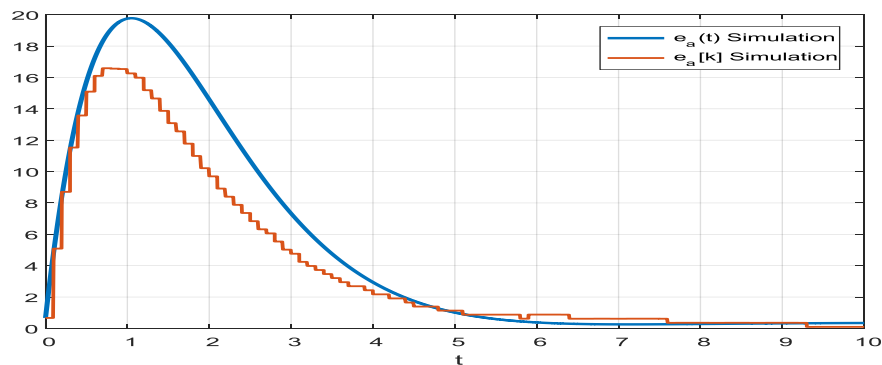


Figure 9: Responses for off-the-manifold dynamics

Figure 10: Feedback linearized input u Figure 11: PMDC motor input voltage e_a

Rapid Control Prototyping(RCP) Setup

The rapid control prototyping (RCP) approach involves Simulink to gather the data from the real-world hardware, like sensor values and system states; analysing, monitor and subsequently issue command to the hardware. This is hardware in loop type strategy, which enables us to update and monitor system variables in the real-time and also enable us to tune the controller parameters in the real time. The hardware components for the RCP operation are shown in Figure 12. A data acquisition card (DAQ) acts as an interface between Simulink and a digital ARM cortex controller attached to the hardware, enabling the Simulink to interface with the hardware. We can not only gather system states from the sensors attached to the controller but also change controller parameters from Simulink. The block diagram that elucidates the RCP mode of operation is shown in Figure 13. The respective sensors data acquisition, signal monitoring and command issue scheme is visible from Figure 13. The hardware interface in Simulink is shown in Figure 14.

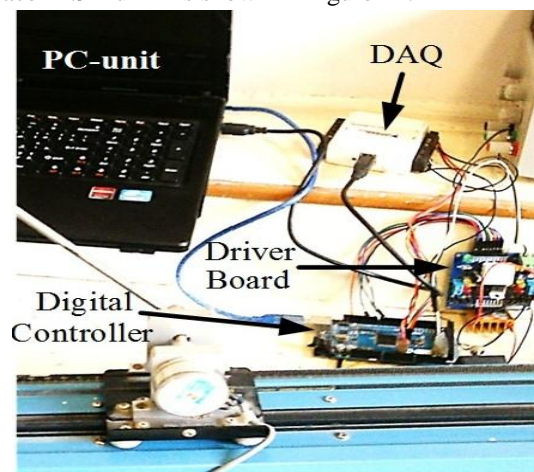


Figure 12: The hardware components for the RCP operation

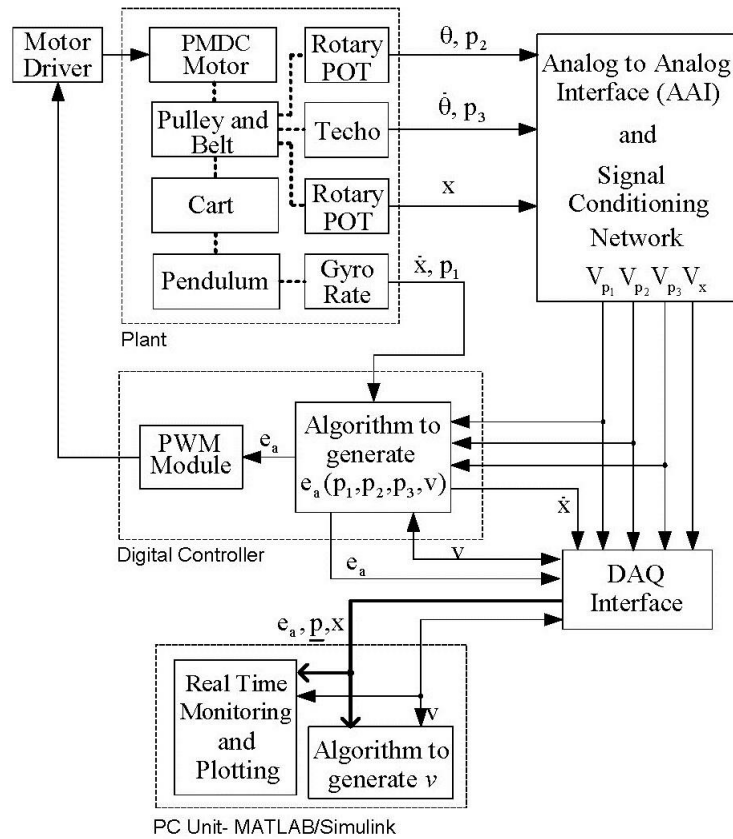


Figure 13: The block diagram for RCP mode of operation

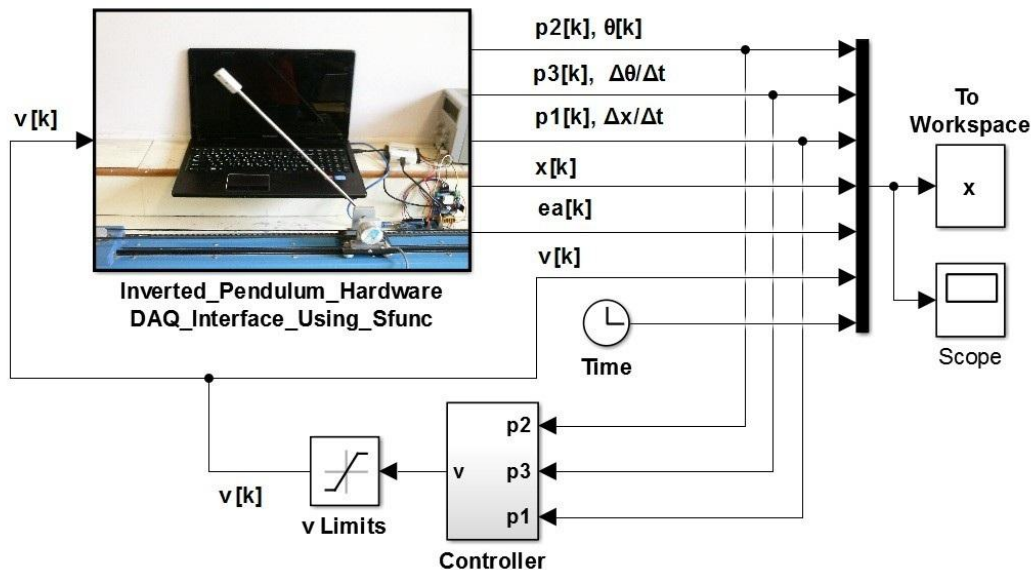


Figure 14: The hardware interface in Simulink

Experimental Results

The digital control algorithm in Equation 6 and Equation 7 is experimentally implemented using Matlab/Simulink in RCP mode. The actual experimental results well follow the simulated system trajectories. For the reference, the continuous time simulation results are also plotted with the experimental results. The pendulum angle and velocity are plotted in the Figure 16 and Figure 17 respectively, and both converge to zero. The cart position and velocity are plotted in Figure 18 and Figure 19 respectively. It is evident that these dynamics are stable. The off-the-manifold dynamics are plotted in Figure 20. These dynamics decay with time

towards zero, hence proving that this submanifold is attractive. The feedback linearized input and PMDC motor input voltages are plotted in Figure 21 and Figure 22 respectively. These values are realizable and within the practical limits.

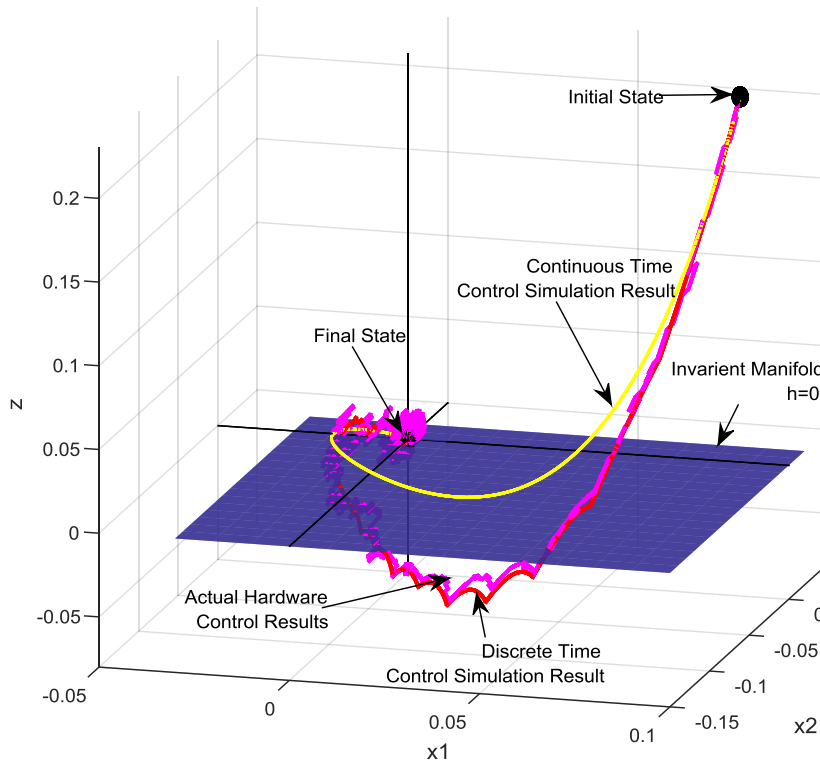


Figure 15: System trajectories and immersion submanifold

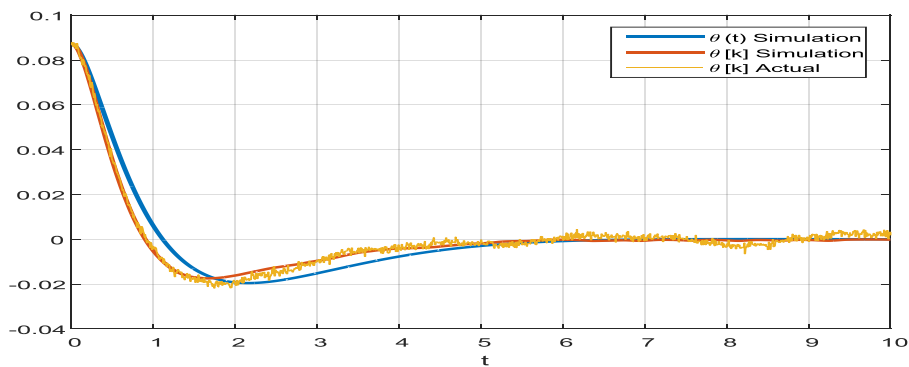


Figure 16: Responses for pendulum angle θ .

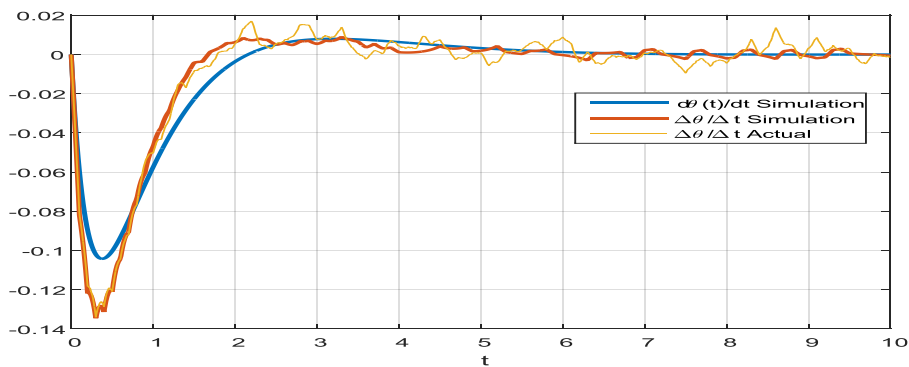


Figure 17: Responses for pendulum angular rates.

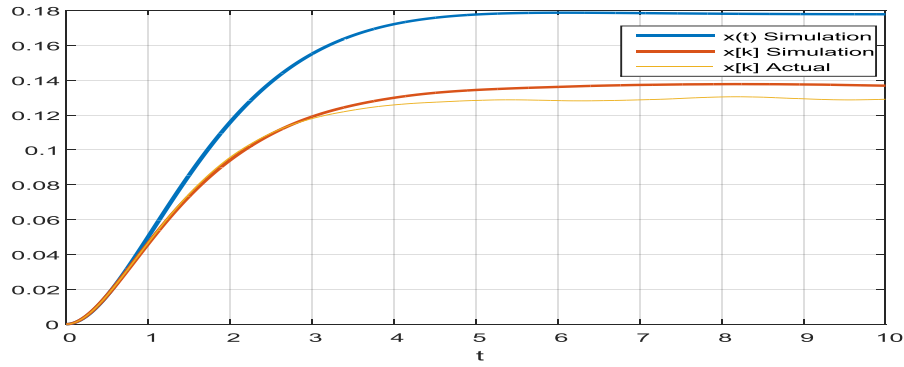


Figure 18: Responses for cart position x .

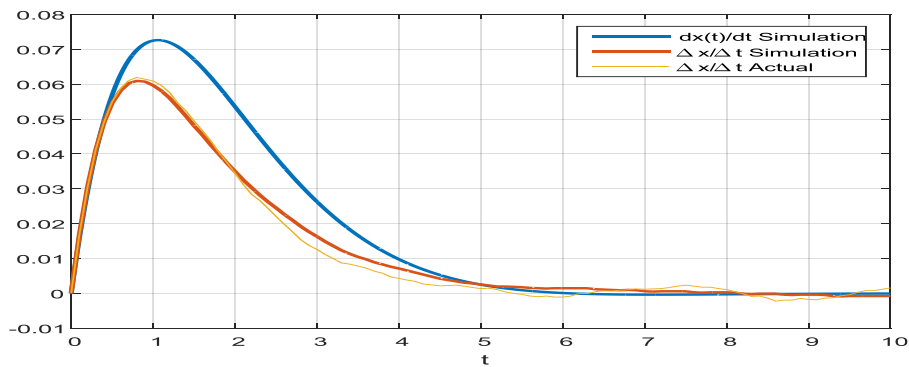


Figure 19: Responses for cart velocity

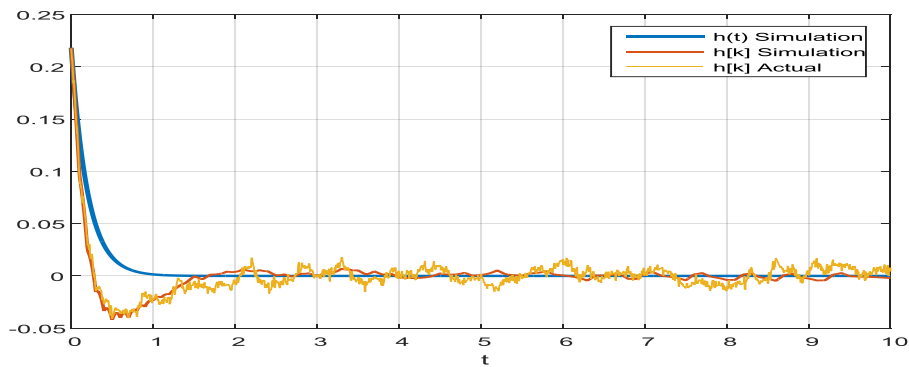


Figure 20: Responses for off-the-manifold dynamics

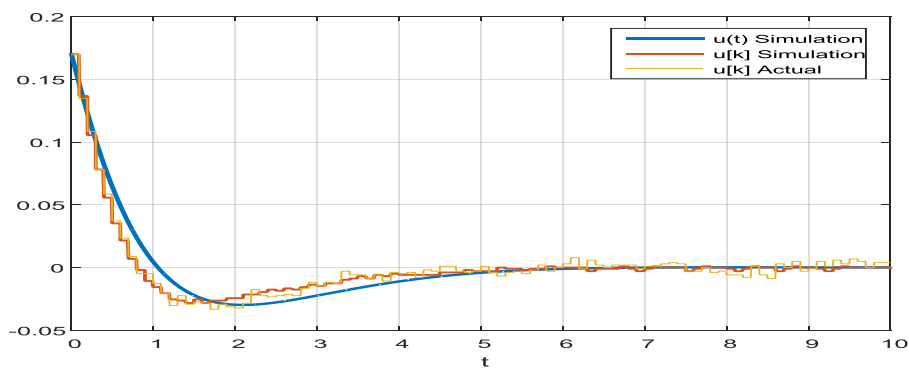


Figure 21: Feedback linearized input u

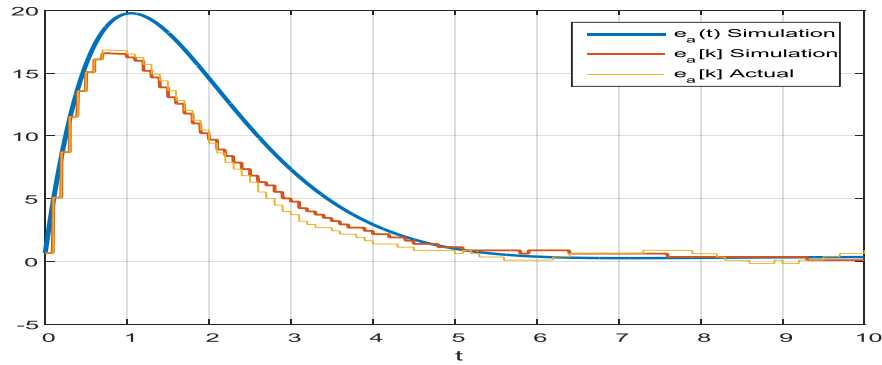


Figure 22: PMDC motor input voltage e_a

Conclusions

The robust adaptive nonlinear control approach for the compensator design of an inverted pendulum has been presented. This approach is successful in attaining the balance of the pendulum, cart position, and velocity with initial conditions of nearly horizontal pendulum angle. The proposed approach provides an immense degree of freedom in selecting the desired closed loop dynamics owing to the availability of free tunable variables in stabilizing control algorithm. Attractively of the submanifold is preserved under digitization of the continuous time control algorithm however invariance property is lost. The experimental results clearly suggest the viability of the proposed controller and defend the position of immersion based adaptive controllers against the classical and many of the modern control approaches, like PID and fuzzy controllers respectively.

References

- [1]. Oróstica.R, Duarte-Mermoud.M.A, and Jáuregui.C, 2016. Stabilization of inverted pendulum using LQR, PID and fractional order PID controllers: A simulated study. *IEEE International Conference on Automatica*, 1-7.
- [2]. Pingale.S.B, Jadhav.S.P, and Khalane.V.P, 2015. Design of fuzzy model reference adaptive controller for inverted pendulum. *International Conference on Information Processing*, 790-794.
- [3]. Jurdjevic.V, 1996. Geometric Control Theory. Cambridge University Press.
- [4]. Astolfi.A, and Ortega.R, 2003. Immersion and invariance: a new tool for stabilization and adaptive control of nonlinear systems. *IEEE Transactions on Automatic Control*, 48(4), 590–606.
- [5]. Grossimon.P.G, Barbieri.E, and Drakuno.S, 1996. Sliding mode control of an inverted pendulum. *IEEE Proceedings of the Twenty-Eighth Southeastern Symposium on System Theory*, 248-252.
- [6]. Luksic.M, Martin.C, and Shadwick.W.F, 1987. Differential Geometry: The Interface between Pure and Applied Mathematics. American Mathematical Society.
- [7]. Prasad.L.B, Tyagi.B, and Gupta.H.O, 2014. Optimal Control of Nonlinear Inverted Pendulum System Using PID Controller and LQR: Performance Analysis Without and With Disturbance Input. *International Journal of Automation and Computing*, 11(6), 661-670.
- [8]. Ming, L. 2012. Self-adaptive fuzzy PID digital control method for linear inverted pendulum. *Proceedings of the 31st Chinese Control Conference*, 3563-3567.
- [9]. Pawar, R. J., and Parvat, B. J. 2015. Design and implementation of MRAC and modified MRAC technique for inverted pendulum. *International Conference on Pervasive Computing*, 1-6.
- [10]. Jung, S., and Kim, S. S. 2007. Hardware Implementation of a Real-Time Neural Network Controller with a DSP and an FPGA for Nonlinear Systems. *IEEE Transactions on Industrial Electronics*, 54(1), 265-271.
- [11]. Mukherjee, S., Pandey, S., Mukhopadhyay, S., and Hui, N. B. 2014. Digital pendulum system: Genetic fuzzy-based online tuning of PID controller. *IEEE 8th International Conference on Intelligent Systems and Control*, 23-28.

